Measurement of Biomechanical Impedance
−Its device and measuring conditions

Hisao OKA* and Tatsuma YAMAMOTO*

SYNOPSIS

Biomechanical impedance is relatively small compared to industrial mechanical impedance. Thus it is difficult to measure it precisely. A biomechanical impedance measuring system was developed for portable use by means of random excitation. This system doesn't require a fixed body and vibrator supporting apparatus. In order to obtain an impedance spectrum, the FFT processing is performed using a personal computer. The spectra of the biomechanical impedance which is measured on body surfaces depend on body positions and can be roughly classified into three spectra patterns : soft, stiff and intermediate. During the measurement, the measuring conditions (preload, diameter of the vibrating tip *etc*.) influence the results. However, it became clear that the linearity of the biomechanical impedance was satisfied in the limited measuring conditions. Accordingly it is possible to standardize the impedance and to compare it with the results under different measuring conditions.

---

* Department of Electrical & Electronic Engineering

1 INTRODUCTION

The body is characterized by having an apparent non-linearity, a complex boundary and a heterogeneous constitution. Its responses are diverse according to the part of the body in question, the duration, frequency and amplitude of vibration. Accordingly, the theoretical analysis of the physical properties of the body is limited. Thus the results of the analysis are only a rough approximation, and since the analysis of the properties is hard to obtain it must have its basis in experimental data.

The mechanical impedance, one of the basic physical properties of the body, can be applied to a linear system theory like electric circuits. Since it is defined only by input and output, the body which has the above mentioned properties can be dealt with by a black-box. Since the biomechanical impedance, however, is relatively small compared to industrial mechanical impedance, it is difficult to measure precisely. Most of the measuring devices[1] of the mechanical impedance which have been reported needed extensive body supporting systems and only certain parts could be measured.

This paper discusses the experimental development of a portable device which can measure the mechanical impedance rapidly in cases of partial excitation whose frequency range is audio (40-1000 Hz). One of the advantage of the portable device is that the measuring can be carried out on any body position. The paper also discusses the mechanical modeling (derived from the impedance measuring of various body parts), which can express the physical properties of the body, and the measuring conditions of the mechanical impedance.

2 MEASUREMENT SYSTEM FOR BIOMECHANICAL IMPEDANCE

It is a common practice to analyze the vibrating characteristics based on the mechanical impedance[2] in the industrial field. The biomechanical impedance is characterized by that its amplitude is relatively small compared to a general mechanical impedance, it is likely to include noise caused by

small body movement and the experimental results on a test sample *in vitro* are not always in agreement with results *in vivo*. Therefore an accurate measurement cannot be expected when an industrial impedance measurement method is applied to biomechanical impedance measurement as it is.

   The biomechanical impedance on a body surface is defined by a driving point impedance between a vibrating force F(f) applied to some driving point and a vibrating velocity V(f) actuated in the direction of F(f).

$$Z(f)=F(f)/V(f)=j\omega F(f)/A(f)=j\omega M(f) \qquad (1)$$

A(f) is an acceleration and M(f) is a complex mass which is a system function between input A(f) and output F(f).

   The exciting force can be chosen from random noise, pseudo-random noise, periodic random noise, periodic impulse, sinusoidal vibration, impact *etc*. These excitations have merits and demerits as regard the duration of measurement and analysis, S/N ratio, control of frequency bandwidth, optimum approximation of non-linearity *etc*.

   When the measuring device of the biomechanical impedance is designed, the exciting force[3] should be selected considering the following conditions. 1) It is desirable to perform the measurement rapidly, since it is impossible to keep a body in a same posture or condition for a long time. 2) Though the body has a linearity within a range of limited input, the non-linearity beyond this range can be suitably approximated linearly. 3) S/N ratio has to be large, because the impedance is relatively small and likely to include a noise caused by a body disturbance. 4) It is possible to change the measuring frequency bandwidth easily. The full consideration of the above points has resulted in a pseudo-random excitation and FFT processing of time response. Then the mechanical impedance is calculated from eqn.1.

2.1 Estimate of system function

   Since the measured input and output are contaminated by

extraneous noise caused by transducer, instrumentation,
computational error etc., the situation is as shown in Fig.1.
$h(\tau)$ is the impulse response function and $H(f)$ is the frequency
response function which corresponds to the complex mass $M(f)$.
$u(t)$ is the input signal, $v(t)$ is the output signal corresponding
to acceleration and force respectively. $m(t)$ and $n(t)$ are noise
signals. In practice the measured signals are the input $a(t)$ and
$b(t)$, or their frequency spectra $A(f)$ and $B(f)$ which include
these noises. Though a true system function is defined by $u(t)$
and $v(t)$, the system function, which is calculated from $a(t)$,
$b(t)$ or $A(f)$, $B(f)$, is contaminated by noise. As the
biomechanical impedance is very small, this noise is one of
factors which influence the measuring accuracy. Some averagings
can minimize the effect of noise. The fundamental equation
relating the input spectrum $A(f)$, the output spectrum $B(f)$ and
the system function $H(f)$ is

$$H(f)=B(f)/A(f)=A^*(f)B(f)/A^*(f)A(f)=S_{AB}(f)/S_{AA}(f) \qquad (2)$$

where * indicates complex conjugation. The autospectrum $S_{AA}(f)$ is
the expected value [ ] of $A^*_i(f)A_i(f)$. Likewise the the
autospectrum $S_{BB}(f)$ is given. The cross spectrum $S_{AB}(f)$ is
defined by $A^*(f)B(f)$.

$$S_{AA}(f)=\lim_{n\to\infty}(1/n)\sum_{i=1}^{n}A^*_i(f)A_i(f)=E[A^*_i(f)A_i(f)] \qquad (3)$$

$$S_{AB}(f)=E[A^*_i(f)B_i(f)] \qquad (4)$$

Instead of $S_{AA}(f)$, $S_{BB}(f)$, and $S_{AB}(f)$, it is more convenient to
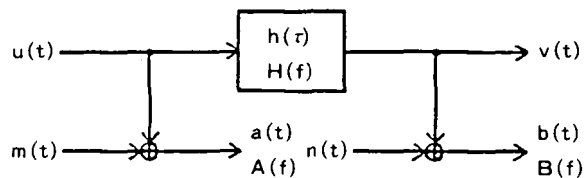work with the corresponding one-sided spectra $G_{AA}(f)$, $G_{BB}(f)$ and

Fig. 1   The system with extraneous noise
in both input and output signals.

$G_{AB}(f)$ defined by

$$H(f)=G_{AB}(f)/G_{AA}(f)=H_1(f) \tag{5}$$

The ratio of these estimates, therefore, gives the frequency response function and is called $H_1(f)$. The ratio of the estimates of $G_{BB}(f)$ and $G_{BA}(f)$ also gives the frequency response function $H(f)$.

$$H(f)=B^*(f)B(f)/B^*(f)A(f)=G_{BB}(f)/G_{BA}(f)=H_2(f) \tag{6}$$

This estimate is called $H_2(f)$. Therefore in the case of the ideal system without extraneous noise, $H_1(f)$ and $H_2(f)$ are called the optimum estimate of $H(f)$ and in the case of a situation with extraneous noise,

$$H_1(f)=H(f)/\{1+G_{MM}(f)/G_{UU}(f)\} \tag{7}$$

$$H_2(f)=H(f)\{1+G_{NN}(f)/G_{VV}(f)\} \tag{8}$$

$$|H_1(f)|<|H(f)|<|H_2(f)| \tag{9}$$

where, $G_{AA}(f)=G_{UU}(f)+G_{MM}(f)$

$$G_{BB}(f)=|H(f)|^2G_{UU}(f)+G_{NN}(f)$$

$$G_{AB}(f)=G_{UV}(f)=H(f)G_{UU}(f)$$

Since the noise signals $m(t)$ and $n(t)$ are assumed to be uncorrelated with each other and with $u(t)$ and $v(t)$, the cross spectra are assumed to be 0 with sufficient averaging. In practice the averaging is performed over only a finite number of records n. In this measurement system n is 16. The phases of $H_1(f)$ and $H_2(f)$ are the same, given by the cross spectrum, but their amplitudes are different. It can be seen that $|H_1(f)|$ underestimates $|H(f)|$ due to the noise at input and that $|H_2(f)|$ overestimates $|H(f)|$ due to the noise at output. Thus $|H_1(f)|$ and

$|H_2(f)|$ are the lower and upper bounds of the true $|H(f)|$. Usually, $H_1(f)$ should be used for the notch amplitudes, where output noise tends to dominate, and $H_2(f)$ at the peak amplitudes, where input noise or leakage tend to cause the problems. In order to get an optimal frequency response function estimate from one measurement, $H_1(f)$ should be used at some frequencies and $H_2(f)$ at other frequencies.

Fig.2 shows the complex masses $|M(f)|$ of the outer forearm at the preload $100g/10mm\phi$, which are calculated from $H_1(f)$ and $H_2(f)$. Thus the complex mass of the body has usually a peak amplitude in low frequency and hardly any notch amplitude. Since both spectra are the same except for the peak amplitude, the complex mass of the body which has only a peak amplitude can be estimated only by $H_2(f)$.

Presence of uncorrelated noise signals is detected by the coherence function $\gamma^2(t)$, but it is not possible to distinguish between input and output noise.

$$\gamma^2(f)=|G_{AB}(f)|^2/\{G_{AA}(f)G_{BB}(f)\}=H_1(f)/H_2(f) \qquad (10)$$

In the above mentioned situation of Fig.1, the coherence is

$$\gamma^2(f)=1/\{1+G_{MM}(f)/G_{UU}(f)\}\{1+G_{NN}(f)/G_{VV}(f)\} \qquad (11)$$

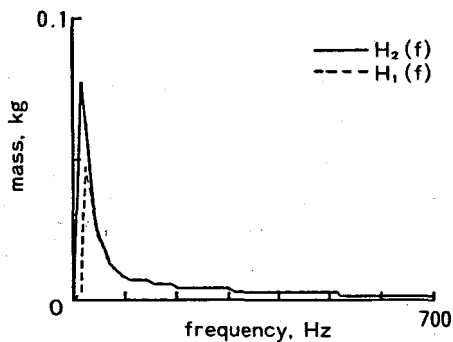If the resolution in the analysis is too coarse compared to the

Fig. 2 $|M(f)|$ calculated from $H_1(f)$ and $H_2(f)$.

bandwidth of the system resonances, and the input signal is random, the coherence function will detect this leakage by having a value less than the one at the resonance frequencies. The expansion of the exciting frequency bandwidth is taken care of.

2.2 Measuring device

Fig.3 shows a block diagram of the measuring device. The vibrator is driven by a random wave, restricted within 1 kHz using an anti-aliasing low-pass filter. The body is vibrated through the vibrating tip placed on the top of the impedance head. A load cell is placed in the vibrating rod in order to read the preload applied to the body surface, because the preload influences the mechanical impedance.

The output signals resulting from random acceleration (A) and stress (F) applied to the body surface, are obtained from the impedance head, amplified by charge amplifiers and sampled by a 12-bit analog-to-digital converter added to personal computer. The FFT processing of both signals is performed with 16 averagings by a personal computer, and finally the complex mass
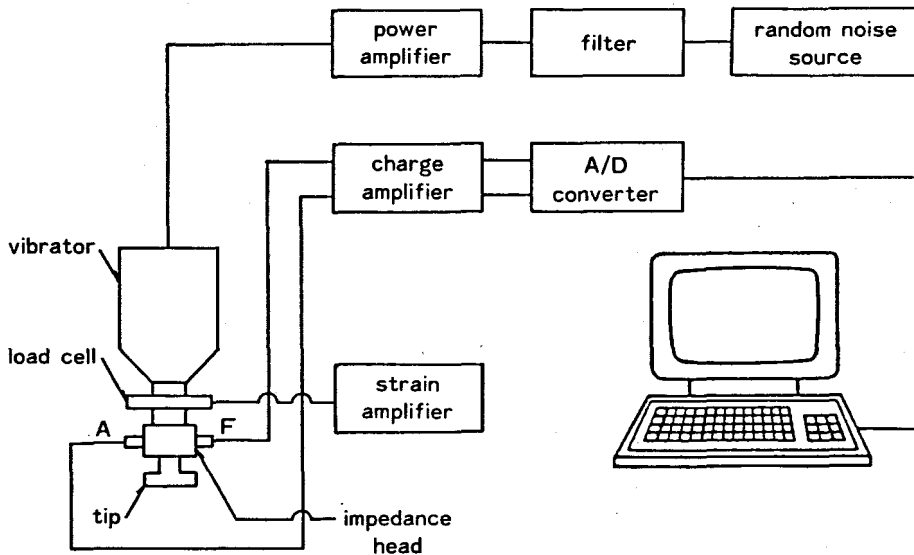

Fig. 3 The measurement system for biomechanical impedance.

and the mechanical impedance are computed by eqn.1.

The FFT processing is performed for 256 data points and the leakage error is minimized by applying a Hanning window to the acceleration and force signal respectively. It takes about only 1.4 seconds (333µs × 256 points × 16 times) to obtain a spectrum below 1 kHz. As the result of the shortened measuring time, a fixed supporting apparatus is unnecessary. Thus it becomes possible to measure on any part of the body without restriction of body positions.

3 MEASUREMENT OF BIOMECHANICAL IMPEDANCE

Generally the biomechanical impedance[4] depends on body positions, measuring conditions (preload, tip diameter, frequency bandwidth) etc. It is difficult to include them in the standardization of biomechanical impedance. Accordingly, measured positions, measuring conditions etc. should be selected.

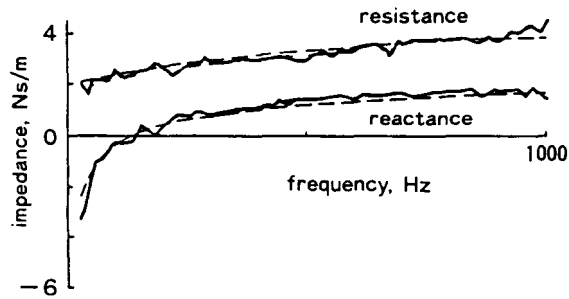### 3.1 Biomechanical impedance spectrum

Since this measuring device adopts a small and light vibrator and impedance head, the measurement system doesn't require a fixed apparatus for supporting the body and vibrator, It becomes possible to measure on any part of the body with the transducer held in one hand. Therefore many body positions, which it has been difficult to measure previously, can be measured[5] and analyzed. The spectra of biomechanical impedance depend on body positions and can be roughly classified into three spectra patterns as shown in Fig.4 (solid lines).

The particular features of Fig.4 are that frequency characteristics of R show a monotonous increase with increasing frequency in a soft tissue, a nearly monotonous decrease in a stiff tissue, and a decrease and increase in an intermediate tissue. The soft and intermediate pattern have resonance frequencies below 1kHz, unlike the stiff pattern. The amplitude of the mechanical impedance (stiffness of movement) is stiff >
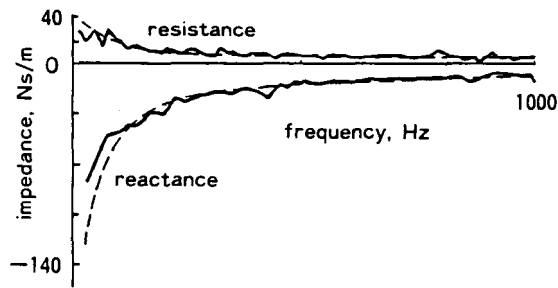
intermediate > soft. The forearm, cheek, palm, throat, pit of stomach and plantar arch are classified as soft pattern. The forehead, tooth and chest (on a rib), as stiff pattern. The gum and temple, as intermediate pattern.
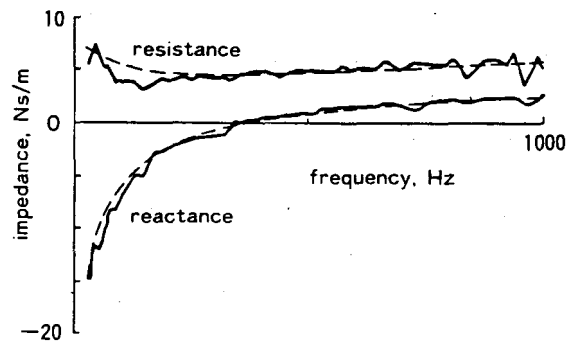
The experimental modeling equations of these impedance spectra

(a) soft

(b) stiff

(c) intermediate

Fig. 4 Three typical biomechanical impedance spectra.

are as follows:

soft pattern ; $Z_s(j\omega)=R_0+(j\omega)^\beta M_0+E_0/j\omega$ (12)

stiff pattern ; $Z_{st}(j\omega)=R_0+K_0/(j\omega)^\alpha+E_0/j\omega$ (13)

intermediate pattern ; $Z(j\omega)=R_0+(j\omega)^\beta M_0+K_0/(j\omega)^\alpha+E_0/j\omega$ (14)

The properties in a soft tissue[6] are composite characteristics of Newtonian viscosity, by which non-Newtonian viscosity due to body fluid is approximated, and a purely elasticity due to a solid part. The properties in a stiff tissue are composite characteristics of a static viscous resistance and a viscoelasticity due to a solid part. The properties in an intermediate tissue are composite characteristics of soft and stiff properties, and they display the characteristics of viscoelasticity due to solid at low frequencies and to approximated Newtonian body fluid at high frequencies. The approximate curves (dotted lines) of the experimental values are determined by these equations by means of curve fitting. They agree with the experimental values and the modeling equations for the three spectra patterns hold to fairly good approximations. The obtained model parameters are shown in Table I.

3.2 Measuring conditions

The biomechanical impedance depends remarkably on the measuring conditions. When the impedance is measured on a surface of the outer forearm in contact with a vibrating tip, the influences of preload and diameter of the vibrating tip have been examined. When the tip diameter changes from 2 to 20mmφ in 5 steps at a fixed pressure of 100g/10mmφ the coefficients of correlation between the tip diameter and mechanical parameters R_0, M_0, E_0 and β are obtained. Likewise the coefficients of correlation are obtained when the preload changes from 20 to 500g in 5 steps at a constant tip diameter 10mmφ. The obtained coefficients are shown in Table II. An adequate correlation is estimated between contact

Table I   Mechanical parameters of some body positions.

Position	R_0 Ns/m	M_0 kgs$^{\beta-1}$	E_0 N/m	K_0 Ns$^{1-\alpha}$/m	α	β
outer forearm	0.898	0.0283	884	–	–	0.572
inner forearm	1.40	0.0377	758	–	–	0.538
palm	3.15	0.182	1300	–	–	0.383
cheek	3.30	0.0117	374	–	–	0.484
lower leg	3.33	0.119	372	–	–	0.386
forehead	1.00	–	52500	5840000	0.999	–
tooth	0.677	–	192000	18800000	0.998	–
knee	2.25	–	18800	2570000	0.998	–
gum	0.190	–	384	1470	0.900	–
nose tip	0.940	0.111	1330	812	0.808	0.460
temple	0.900	0.0786	272	3920	0.792	0.490

Table II   Coefficients of correlation between mechanical parameters and contact area, pressure.

	R_0	M_0	E_0	β
area	0.94	0.64	0.94	0.97
pressure	0.98	0.43	0.96	0.44

area and mechanical parameters, but a lower correlation between contact pressure and mechanical parameters. The linearity between impedance spectrum and contact area S, pressure P is discussed.

Fig.5 shows the mechanical resistance R_0 and reactance X_0 of outer forearm at a fixed pressure (150g/cm^2) using 3 tips (5, 10, 15mm). $Z_0=R_0+jX_0$ is an impedance Z/S per unit area. Three spectra are slightly scattered but can be approximately estimated to be $Z=SZ_0$. The linearity is satisfied in this range.

Fig.6 shows the impedance spectra of the outer forearm at 3 pressures (100, 200, 300g/cm^2). Since the three spectra are
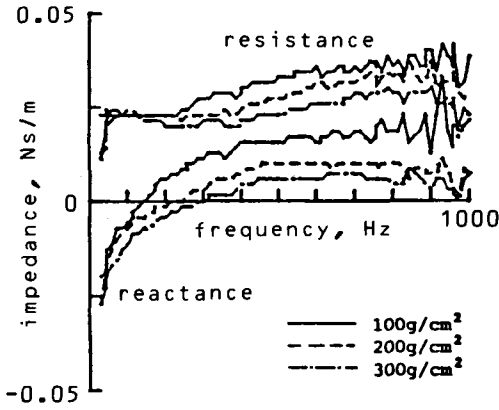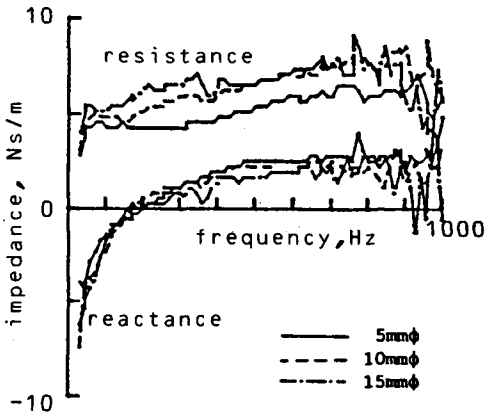
Fig. 5 Biomechanical impedance
per unit area.
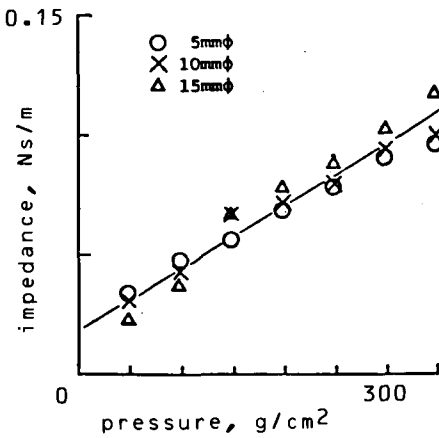
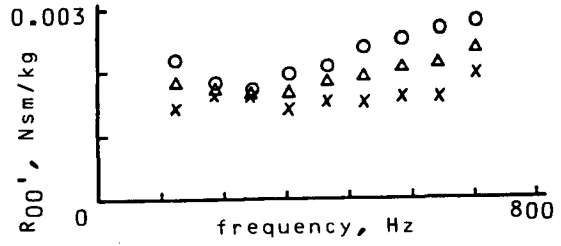

Fig. 6 Biomechanical impedance
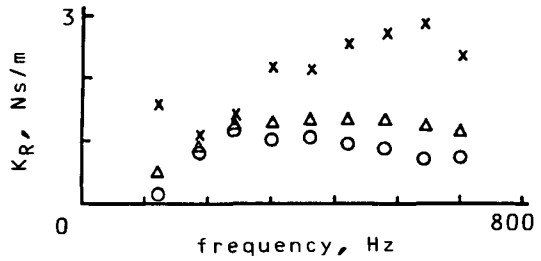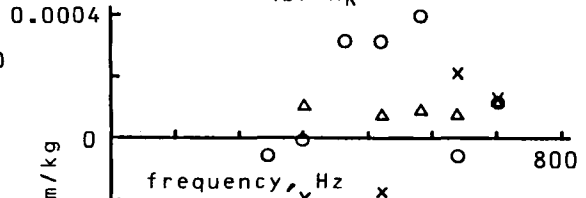per unit pressure.

Fig. 8 The relation between the
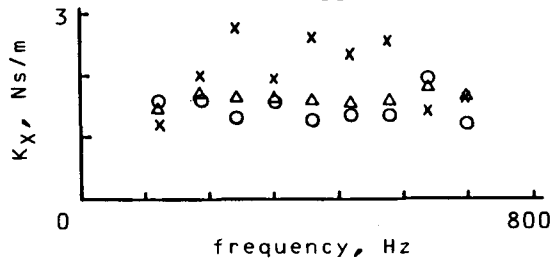impedance per unit area and
contact pressure.

(a) R_{00}'

(b) K_R

(c) X_{00}'

(d) K_X

Fig. 7 The linearity of mechanical
impedance in contact pressure.
(o:100-200,×:200-300,△:300-100g/cm²)

nearly the same, they are possible to express by $R = PR_{00}' + K_R$ and $X = PX_{00}' + K_X$. Fig.7(a)-(d) shows R_{00}', X_{00}', K_R and K_X in 200-700 Hz. The parameters obtained at $200-300 g/cm^2$ are slightly different but the linearity seems to be satisfied in this range.

Fig.8 shows a mean impedance per unit area $|\overline{z}|_0 = |\overline{z}|/S$. $|\overline{z}|$ is a mean impedance of absolute impedance value $|z|$ of the outer forearm. Since $|\overline{z}|_0$ is closely approximated by $0.025P + 0.02$, the linearity is satisfied in the range of lower pressure below $300 g/cm^2$. It became clear that the linearity of the biomechanical impedance was satisfied in the limited measuring conditions. Accordingly it is possible to standardize the impedance measured in this range and to compare with the results under different measuring conditions.

This paper discussed experimentally the effects of measuring conditions. On the other hand, Franke[7] made a theoretical analysis of the relation between a mechanical impedance and contact area on the soft tissue using the mathematical model. Vermarien[8] et al. explained the loading effect on the chest wall with Norton's theorem and Thévenin's law using the coupling model.

4 CONCLUSIONS

This paper deals mainly with the development of biomechanical impedance measurement and its measuring conditions. Though the biomechanical impedance is relatively small compared to machinery impedance, and it is difficult to measure precisely, a measurement method and its measuring device with random excitation have been developed. Since the measuring device is for portable use and not expensive, it becomes possible to measure on any body position and easy to accumulate clinical data.

The biomechanical impedance of some body positions are measured and roughly classified into three spectra patterns. The measuring conditions of impedance also are discussed. Consequently the new clinical applications for biomechanical impedance are anticipated.

REFERENCES

(1)T. J. Moore, IEEE Trans., <u>MMS-11</u>(1970), 79.

(2)C. M. Harris and C. E. Crede, "Shock & Vibration Handbook" (Second Edition), McGraw-HILL (1976), 10-1.

(3)H. Oka and T. Yamamoto, Innov. Tech. Biol. Med., <u>8</u>(1987), 1.

(4)H. E. von Gierke, H. L. Oestreicher, E. K. Franke, H. O. Parrack and W. W. von Wittern, J. Appl. Physiol., <u>4</u>(1952), 886.

(5)T. Yamamoto and H. Oka, Med. & Biol. Eng. & Comput., <u>24</u>(1986), 493.

(6)H. Oka and T. Yamamoto, Med. & Biol. Eng. & Comput., <u>25</u>(1987), 631.

(7)E. K. Franke, J. Appl. Physiol., <u>3</u>(1951), 582.

(8)H. Vermarien and E. van Vollenhoven, Med. & Biol. Eng. & Comput., <u>22</u>(1984), 168.